

Soil carbon loss by experimental warming in a tropical forest

<https://doi.org/10.1038/s41586-020-2566-4>

Andrew T. Nottingham^{1,2}, Patrick Meir^{1,3}, Esther Velasquez² & Benjamin L. Turner²

Received: 7 June 2019

Accepted: 18 June 2020

Published online: 12 August 2020

 Check for updates

Tropical soils contain one-third of the carbon stored in soils globally¹, so destabilization of soil organic matter caused by the warming predicted for tropical regions this century² could accelerate climate change by releasing additional carbon dioxide (CO_2) to the atmosphere^{3–6}. Theory predicts that warming should cause only modest carbon loss from tropical soils relative to those at higher latitudes^{5,7}, but there have been no warming experiments in tropical forests to test this⁸. Here we show that *in situ* experimental warming of a lowland tropical forest soil on Barro Colorado Island, Panama, caused an unexpectedly large increase in soil CO_2 emissions. Two years of warming of the whole soil profile by four degrees Celsius increased CO_2 emissions by 55 per cent compared to soils at ambient temperature. The additional CO_2 originated from heterotrophic rather than autotrophic sources, and equated to a loss of 8.2 ± 4.2 (one standard error) tonnes of carbon per hectare per year from the breakdown of soil organic matter. During this time, we detected no acclimation of respiration rates, no thermal compensation or change in the temperature sensitivity of enzyme activities, and no change in microbial carbon-use efficiency. These results demonstrate that soil carbon in tropical forests is highly sensitive to warming, creating a potentially substantial positive feedback to climate change.

Tropical forests have a large role in the global carbon cycle because they exchange more CO_2 with the atmosphere than any other ecosystem, contain roughly two-thirds of terrestrial plant biomass⁹ and harbour a substantial fraction of global soil carbon¹. Between 30% and 50% of the carbon respired from tropical forests originates from soil, most of which is derived from the decomposition of organic matter^{10–12}. Thus, even a small increase in respiration from tropical forest soils could have a large effect on atmospheric CO_2 concentrations, with consequences for global climate.

There is considerable concern that increased global temperatures will destabilize soil carbon and increase the flux of CO_2 from soil to the atmosphere^{3–6}. Experiments in temperate and arctic regions have consistently found that short-term warming causes a considerable increase in soil CO_2 efflux compared to soil at ambient temperature^{3,6,13} (for example, a 37% increase over 2 years in temperate forest)⁶. For the tropics, the response of soil carbon to warming is expected to be smaller than at higher latitudes because kinetic theory predicts that the intrinsic temperature sensitivity of reaction rates is reduced at higher temperatures^{5,14}. Consistent with this, a meta-analysis of warming experiments has shown that the temperature sensitivity of soil CO_2 efflux increases with latitude⁷. However, the extent to which intrinsic temperature sensitivity translates into actual ('apparent') temperature sensitivity depends on covariation of other environmental factors that influence respiration, such as soil moisture and substrate availability^{5,15}. As there have been no *in situ* warming experiments conducted in tropical forests, the apparent temperature sensitivity of soil organic matter in this biome remains unknown. As a result, earth system models

continue to use kinetic theory to define the temperature sensitivity of soil carbon in the tropics¹⁶, limiting how well they predict the response of tropical forests to global environmental change^{17,18}.

Several factors could influence the apparent temperature sensitivity of soil organic matter. For example, soil warming is typically accompanied by soil drying, which can either reduce respiration in aerobic soils by reducing water availability, or increase respiration in waterlogged soils by increasing oxygen availability^{5,8,15}. Warming can also affect respiration rates by inducing changes in biotic processes, such as the physiology or community composition of microbes, or changes in substrate availability to decomposers¹⁴. In experiments performed at higher latitudes, temperature-adaptive or compensatory responses of microbial communities and enzyme activities have been shown to modulate the effect of warming on the soil carbon cycle^{3,14}. In the tropics, future new temperature maxima could exceed critical biochemical thresholds^{8,19,20}, with added complexity emerging from altered interactions among species-rich plant and microbial communities²¹ and covarying changes in hydrological or nutrient cycles⁸.

Here we present results from the first whole-soil-profile warming experiment in a tropical forest (SWELTR: Soil Warming Experiment in Lowland Tropical Rainforest). The experiment tests the response of the whole soil profile to the 4 °C warming predicted for tropical latitudes by the end of this century¹⁷ (Fig. 1a, Extended Data Figs. 1, 2). SWELTR consists of five pairs of circular control and warmed plots distributed evenly within approximately 1 ha of semideciduous moist lowland tropical forest on Barro Colorado Island, Panama. The soils are moderately weathered Dystric Eutrudepts (Inceptisols)

¹School of Geosciences, University of Edinburgh, Edinburgh, UK. ²Smithsonian Tropical Research Institute, Panama City, Panama. ³Research School of Biology, Australian National University, Canberra, Australian Capital Territory, Australia. [✉]e-mail: Andrew.Notttingham@ed.ac.uk

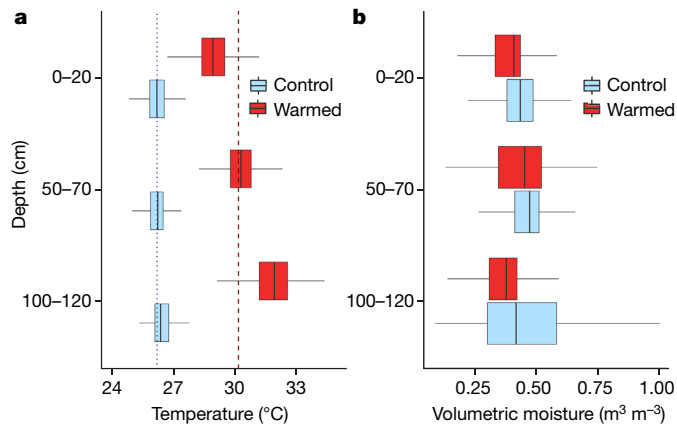


Fig. 1 | Soil temperature and moisture content in control and warmed plots by depth. **a**, Soil temperature. **b**, Volumetric soil moisture content. Data are measurements from integrated soil temperature and moisture probes for the two-year period after the warming treatment began (December 2016 to December 2018). The vertical lines in **a** (dotted blue and dashed red) show the mean soil temperature across the soil profile, which is 26.18 °C for control plots and 30.14 °C for warmed plots (3.96 °C difference). The treatment effect was $P < 0.001$ for all comparisons, based on the temporal variation across $n = 5$ plots. Box plots are standard Tukey plots, where the centre line represents the median, the lower and upper hinges represent the first and third quartiles, and whiskers represent ± 1.5 the interquartile range. The treatments are offset on the y axis (depth) for easier viewing.

that have developed on the volcanic facies of the Bohio formation (Extended Data Table 1, Methods). Each warmed plot has a ground surface area of around 20 m² heated to 1.2 m depth, resulting in a total volume of 120 m³ of warmed soil across the experiment.

Two years of experimental warming increased soil CO₂ emissions by 55%, from 18.8 ± 1.9 megagrams of carbon per hectare per year (Mg C ha⁻¹ yr⁻¹) in control plots to 29.2 ± 5.0 Mg C ha⁻¹ yr⁻¹ in warmed plots (treatment effect, $P < 0.05$; Fig. 2, Extended Data Table 2, Extended Data Fig. 3). The soil CO₂ emission rate from unheated (control) plots is representative of tropical forests worldwide (8–40 Mg C ha⁻¹ yr⁻¹), including in the Amazon basin (12–24 Mg C ha⁻¹ yr⁻¹)²². Using exclusion and ingrowth cores to partition respiration from heterotrophic (soil-derived) and autotrophic (root-derived) sources, we find that the increase in CO₂ efflux was derived predominantly from heterotrophic sources, whether from the decomposition of leaf-litter inputs or from pre-existing soil organic matter (Figs. 2, 3, Extended Data Fig. 4). Soil-derived respiration increased from 12.0 ± 2.1 Mg C ha⁻¹ yr⁻¹ in control plots to 20.1 ± 4.2 Mg C ha⁻¹ yr⁻¹ in warmed plots (a 68% increase of 8.2 Mg C ha⁻¹ yr⁻¹; treatment effect, $P < 0.05$), whereas root-derived respiration was not altered significantly ($P = 0.21$; 6.8 ± 1.2 Mg C ha⁻¹ yr⁻¹ and 9.0 ± 3.4 Mg C ha⁻¹ yr⁻¹ in control and warmed plots, respectively; Fig. 3, Extended Data Table 3).

It is possible that the large warming-induced increase in soil CO₂ efflux was due in part to soil drying because the warmed plots were slightly drier than the controls, particularly in the early wet season (Extended Data Fig. 2). In very wet soils, soil drying can increase respiration by increasing the supply of oxygen to microbes. By contrast, soil drying under aerobic conditions can reduce heterotrophic respiration by promoting water limitation of microbial metabolism²⁰. Here, we find a marginally non-significant effect of soil moisture on CO₂ efflux across seasons (Extended Data Table 2; annual, $P = 0.69$; wet-season, $P = 0.07$; dry-season, $P = 0.06$), consistent with the parabolic relationship of CO₂ efflux with soil moisture for this site²². However, there was no direct effect of warming on soil moisture (surface soils, $P = 0.19$; whole-profile, $P = 0.24$; Extended Data Table 4) and the interaction between soil moisture and warming in the CO₂ efflux model was not

significant (annually and for individual seasons; $P > 0.2$; Extended Data Table 2), indicating that the warming effect on CO₂ efflux was not influenced by soil moisture. Furthermore, soil moisture was not correlated with soil CO₂ efflux in the warmed plots (Extended Data Fig. 3), and drying during the early wet season in warmed soil (Extended Data Fig. 2) should decrease rather than increase CO₂ efflux because the soil was aerobic during this period and below the moisture content of 0.45 m³ m⁻³ at which soil CO₂ efflux peaks in this forest²². Our data thus show that although soil moisture influenced soil CO₂ efflux and that warmed plots were slightly drier than control plots, particularly during the early wet season, this did not contribute significantly to the increased CO₂ efflux from the warmed soil.

There was no moderation of the warming-induced increase in soil CO₂ efflux over the two years of the experiment. Such a moderation might be expected in the long-term, through substrate limitation, adaptation of microbial communities (through changes in microbial carbon-use efficiency; CUE) or thermal compensation of enzyme activities (reduced maximum potential activity (V_{max}) at higher temperatures)^{3,14,23}. We found no reduction in extractable or mineralized nitrogen or phosphorus with warming, as would be expected under nutrient limitation (Extended Data Fig. 5). Almost all hydrolytic enzymes were unaffected by warming (Extended Data Fig. 5), except for β -xylanase (an enzyme involved in hemicellulose degradation), for which activity increased with warming during the wet season—an opposite response to that predicted by thermal compensation¹⁹. The temperature sensitivity of enzyme activity (Q_{10} of V_{max}) was unaffected by warming (Extended Data Fig. 5a), indicating no dampening effect on soil carbon breakdown via thermal adaptation of enzyme production as expected at warmer temperatures²⁴. Microbial CUE, which broadly represents carbon stabilized in biomass relative to carbon lost in respiration and can influence long-term (decadal) soil carbon loss^{3,23}, was unaffected by warming (treatment effect, $P = 0.37$; Extended Data Fig. 5). Microbial biomass carbon, however, increased with warming at the annual scale (treatment effect, annual scale, $P = 0.02$), with a marginally non-significant increase at the seasonal scale ($P < 0.1$; Extended Data Fig. 5). Together, these results suggest slightly increased growth in response to greater organic-matter turnover in the absence of nutrient constraints to carbon degradation, which did not translate into changes in CUE.

Our finding that tropical forest soil carbon has a high apparent temperature sensitivity challenges the prevailing expectation that the temperature sensitivity of soil carbon is lower in the tropics compared to cooler ecosystems at higher latitudes^{5,7}. The 55% increase in total soil CO₂ emissions we report here (from 18.8 to 29.2 Mg C ha⁻¹ yr⁻¹) following two years of 4 °C whole-soil-profile warming is larger than that found in a temperate forest using a similar whole-profile experimental design (34%–37% increase over two years of 4 °C whole-profile warming, from 13.0 to 17.5 Mg C ha⁻¹ yr⁻¹)⁶. Furthermore, the rate of additional soil carbon loss (8.2 Mg C ha⁻¹ yr⁻¹) is greater than for all the studies in a recent meta-analysis of surface-only soil warming experiments at higher-latitude sites (all loss rates less than 5 Mg C ha⁻¹ yr⁻¹)⁴. The expectation that the temperature sensitivity of soil carbon breakdown is lower in the tropics compared to higher latitudes, based in part on kinetic theory and commonly used to describe soil carbon responses in earth system models¹⁶, is therefore not consistent with the ('apparent')^{5,15} temperature sensitivity of the breakdown of tropical forest soil carbon reported here. However, our results are consistent with recent atmospheric and satellite measurements, which have shown a high sensitivity of ecosystem-scale carbon cycling in tropical regions in response to interannual temperature variation^{25,26}. Our findings suggest that tropical soils contribute substantially to these ecosystem-scale responses to warming.

This high apparent temperature sensitivity of tropical forest soil carbon under in situ experimental warming must arise through the temperature response of covarying ecosystem properties rather than as

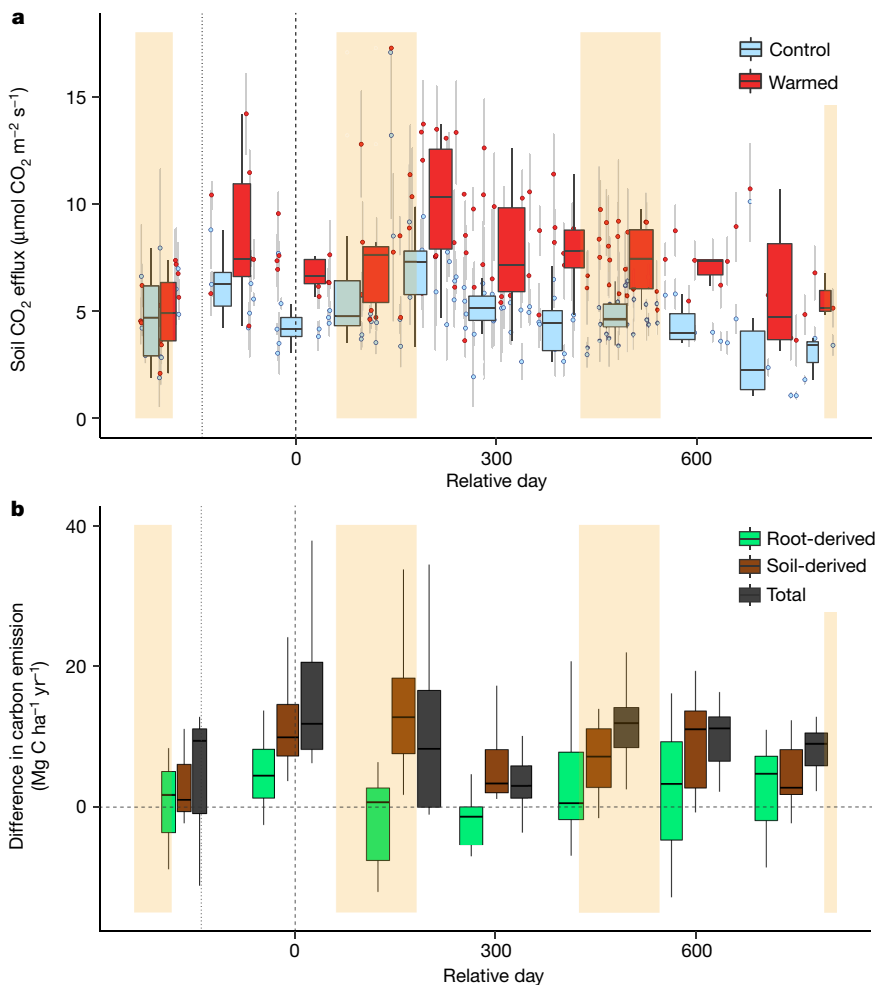


Fig. 2 | Soil CO₂ efflux from control and warmed soils over two years. **a**, Total soil CO₂ flux during the study period (2017–2019), relative to the beginning of the warming treatment (relative day 0). **b**, Difference in carbon emission (warmed minus control) partitioned into soil-derived and root-derived components. Measurements were made every two weeks. Points in **a** represent the mean value of five plots, with error bars representing one standard error of the spatial variation ($n = 5$ plots). The box plots represent the temporal variation over sequential 100-day periods to show seasonal dynamics. Box plots are standard Tukey plots, where the centre line represents the median, the lower and upper hinges represent the first and third quartiles, and whiskers represent +1.5 the interquartile range. The dotted vertical line shows when installation and testing of warming plots began (during this period each plot was warmed by 4 °C relative to controls for a period of 1–2 weeks); the dashed vertical line (relative day 0; 1 November 2017) shows when all five warming plots were switched on permanently. The yellow shaded areas represent dry seasons (1 January to 1 April). Soil CO₂ efflux was significantly higher in warmed plots for annual data and for dry or wet seasons individually (Extended Data Table 2).

the sole consequence of intrinsic kinetic processes. Although our data do not provide conclusive evidence for the mechanism(s) underlying this marked increase in soil carbon loss from warmed soil, several findings point to a possible explanation: (i) the general absence of thermal compensation in enzyme activities (no decrease in V_{\max}); (ii) the lack of change in the temperature sensitivity of enzymes under warming (no decrease in Q_{10} of V_{\max}); and (iii) the lack of a moderating thermal

response of microbial CUE (Extended Data Fig. 5)^{23,27,28}. Together, our results indicate that organic-matter degradation increased under warming with no moderating responses or acclimation among microbial communities or the enzymes they synthesize.

This surprisingly large loss of soil carbon from warmed soil represents a substantial positive climate feedback over the period of this study. The additional carbon loss from warming observed here

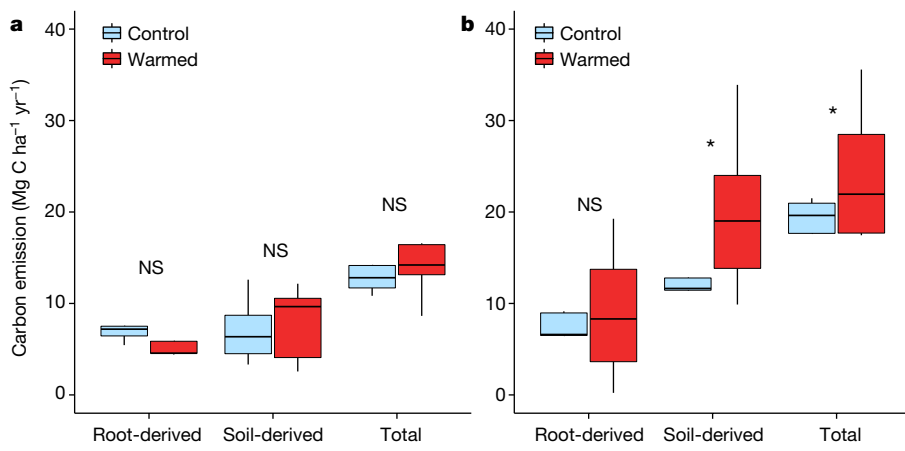


Fig. 3 | The annual carbon emission partitioned into soil-derived and root-derived components. **a**, The pre-treatment period (January–May 2016; predominantly dry season). **b**, The two years with warming. The figures show total CO₂ and the root-derived and soil-derived components calculated using CO₂ efflux from partition cores (equations (1) and (2) in Methods). Differences

between control and warmed plots are shown by asterisks where $P \leq 0.05$ or as non-significant (NS); determined using mixed effect models (Extended Data Tables 2, 3). Box plots are standard Tukey plots, where the centre line represents the median, the lower and upper hinges represent the first and third quartiles, and whiskers represent +1.5 the interquartile range (for $n = 5$ plots).

is of similar magnitude to annual carbon input from litterfall at this site ($5\text{--}7 \text{ Mg C ha}^{-1} \text{ yr}^{-1}$)²⁹ and is equivalent to approximately 13% of the total soil carbon stock, or 30% of gross primary productivity ($27.5 \text{ Mg C ha}^{-1} \text{ yr}^{-1}$)³⁰. Extrapolation of the first two years of carbon loss in our experiment across the entire tropical forest soil carbon stock (502 Pg C)¹ indicates a global loss of more than 65 Pg C with 4°C warming this century, which is in broad agreement with estimated carbon loss based on a five-year soil translocation experiment in tropical forests elsewhere³¹. In light of these findings, earlier estimates of global soil carbon loss under 4°C warming (110–190 Pg C)^{3,32}, which were based on experiments performed at higher latitudes, underestimate the magnitude of this global earth–atmosphere feedback.

We expect that the rate of soil carbon loss will eventually decline in warmed soils as substrate limitation increases, but we do not know how long this will take, nor whether the long-term soil carbon balance will be affected by plant–soil interactions or changes in soil microbial communities as they adapt to warmer temperatures^{3,13,14,23}. The nature of these longer-term responses will determine the strength of this positive earth–atmosphere feedback, which is already substantial in the short-term, in contributing to further climate warming.

Online content

Any methods, additional references, Nature Research reporting summaries, source data, extended data, supplementary information, acknowledgements, peer review information; details of author contributions and competing interests; and statements of data and code availability are available at <https://doi.org/10.1038/s41586-020-2566-4>.

1. Jackson, R. B. et al. The ecology of soil carbon: pools, vulnerabilities, and biotic and abiotic controls. *Annu. Rev. Ecol. Evol. Syst.* **48**, 419–445 (2017).
2. Ciais, P. et al. in *Climate Change 2013: The Physical Science Basis. Contribution of Working Group I to the Fifth Assessment Report of the Intergovernmental Panel on Climate Change* (eds Stocker, T. F. et al.) Ch. 6 (Cambridge Univ. Press, 2013).
3. Melillo, J. M. et al. Long-term pattern and magnitude of soil carbon feedback to the climate system in a warming world. *Science* **358**, 101–105 (2017).
4. van Gestel, N. et al. Predicting soil carbon loss with warming. *Nature* **554**, E4–E5 (2018).
5. Davidson, E. A. & Janssens, I. A. Temperature sensitivity of soil carbon decomposition and feedbacks to climate change. *Nature* **440**, 165–173 (2006).
6. Hicks Pries, C. E., Castanha, C., Porras, R. C. & Torn, M. S. The whole-soil carbon flux in response to warming. *Science* **355**, 1420–1423 (2017).
7. Carey, J. C. et al. Temperature response of soil respiration largely unaltered with experimental warming. *Proc. Natl Acad. Sci. USA* **113**, 13797–13802 (2016).
8. Wood, T. E. et al. in *Ecosystem Consequences of Soil Warming: Microbes, Vegetation, Fauna and Soil Biogeochemistry* (ed. Mohan, J. E.) Ch. 14, 385–439 (Academic Press, 2019).
9. Pan, Y. et al. A large and persistent carbon sink in the world's forests. *Science* **333**, 988–993 (2011).
10. Anderson-Teixeira, K. J., Wang, M. M. H., McGarvey, J. C. & LeBauer, D. S. Carbon dynamics of mature and regrowth tropical forests derived from a pantropical database (TropForC-db). *Glob. Change Biol.* **22**, 1690–1709 (2016).
11. Malhi, Y. The productivity, metabolism and carbon cycle of tropical forest vegetation. *J. Ecol.* **100**, 65–75 (2012).
12. Chambers, J. Q. et al. Respiration from a tropical forest ecosystem: partitioning of sources and low carbon use efficiency. *Ecol. Appl.* **14**, 72–88 (2004).
13. Romero-Olivares, A. L., Allison, S. D. & Treseder, K. K. Soil microbes and their response to experimental warming over time: a meta-analysis of field studies. *Soil Biol. Biochem.* **107**, 32–40 (2017).
14. Tang, J. et al. in *Ecosystem Consequences of Soil Warming: Microbes, Vegetation, Fauna and Soil Biogeochemistry* (ed. Mohan, J. E.) Ch. 8, 175–201 (Academic Press, 2019).
15. Nottingham, A. T. et al. Climate warming and soil carbon in tropical forests: insights from an elevation gradient in the Peruvian Andes. *Bioscience* **65**, 906–921 (2015).
16. Todd-Brown, K. E. O. et al. Causes of variation in soil carbon predictions from CMIP5 Earth system models and comparison with observations. *Biogeosciences* **10**, 1717–1736 (2013).
17. Intergovernmental Panel on Climate Change (IPCC). *Global Warming of 1.5°C: An IPCC Special Report on the Impacts of Global Warming of 1.5°C Above Pre-Industrial Levels and Related Global Greenhouse Gas Emission Pathways, in the Context of Strengthening the Global Response to the Threat of Climate Change, Sustainable Development, and Efforts to Eradicate Poverty* (eds Masson-Delmotte, V. et al.) Ch. 3 (World Meteorological Organization, 2018).
18. Cox, P. M. et al. Sensitivity of tropical carbon to climate change constrained by carbon dioxide variability. *Nature* **494**, 341–344 (2013).
19. Mora, C. et al. The projected timing of climate departure from recent variability. *Nature* **502**, 183–187 (2013).
20. Beaumont, L. J. et al. Impacts of climate change on the world's most exceptional ecoregions. *Proc. Natl Acad. Sci. USA* **108**, 2306–2311 (2011).
21. Steidinger, B. S. et al. Climatic controls of decomposition drive the global biogeography of forest-tree symbioses. *Nature* **569**, 404–408 (2019).
22. Rubio, V. E. & Detto, M. Spatiotemporal variability of soil respiration in a seasonal tropical forest. *Ecol. Evol.* **7**, 7104–7116 (2017).
23. Frey, S. D., Lee, J., Melillo, J. M. & Six, J. The temperature response of soil microbial efficiency and its feedback to climate. *Nat. Clim. Chang.* **3**, 395–398 (2013).
24. Bradford, M. A. Thermal adaptation of decomposer communities in warming soils. *Front. Microbiol.* **4**, <https://doi.org/10.3389/fmicb.2013.00333> (2013).
25. Wang, X. H. et al. A two-fold increase of carbon cycle sensitivity to tropical temperature variations. *Nature* **506**, 212–215 (2014).
26. Liu, J. J. et al. Contrasting carbon cycle responses of the tropical continents to the 2015–2016 El Niño. *Science* **358**, eaam5690 (2017).
27. Karhu, K. et al. Temperature sensitivity of soil respiration rates enhanced by microbial community response. *Nature* **513**, 81–84 (2014).
28. Bradford, M. A. et al. Cross-biome patterns in soil microbial respiration predictable from evolutionary theory on thermal adaptation. *Nat. Ecol. Evol.* **3**, 223–231 (2019).
29. Wieder, R. K. & Wright, S. J. Tropical forest litter dynamics and dry season irrigation on Barro Colorado Island, Panama. *Ecology* **76**, 1971–1979 (1995).
30. Chave, J. et al. Spatial and temporal variation of biomass in a tropical forest: results from a large census plot in Panama. *J. Ecol.* **91**, 240–252 (2003).
31. Nottingham, A. T. et al. Microbial responses to warming enhance soil carbon loss following translocation across a tropical forest elevation gradient. *Ecol. Lett.* **22**, 1889–1899 (2019).
32. Crowther, T. W. et al. Quantifying global soil carbon losses in response to warming. *Nature* **540**, 104–108 (2016).

Publisher's note Springer Nature remains neutral with regard to jurisdictional claims in published maps and institutional affiliations.

© The Author(s), under exclusive licence to Springer Nature Limited 2020

Article

Methods

Site and experiment

The experiment is situated in approximately 1 ha of seasonally moist lowland tropical forest on Barro Colorado Island, Panama³³. Within the plot area, the dominant tree species include *Anacardium excelsum* and *Poulsenia armata*. The soils are Inceptisols (fine, isohyperthermic, Dystric Eutropepts) that are rich in clay (about 54% profile-weighted clay concentration) and secondary metal oxides. They are developed on the volcanic facies of the Bohio formation, a basaltic conglomerate of Oligocene age³⁴. Although these moderately weathered Inceptisols are less infertile than soils under larger areas of lowland tropical forests, Inceptisols still account for 14% of total land area in the tropics (Ultisols and Oxisols account for 20% and 23%, respectively)³⁵, and soil respiration in the control plots in our experiment is comparable to that in lowland tropical forests in general, including those on Ultisols and Oxisols²².

The SWELTR experiment consists of ten circular plots (five paired 'warm' and 'control' plots). Each plot measures 5 m diameter, with approximately 10 m between each pair of control and warmed plots and a minimum of 20 m between different plot pairs. The warmed plots contain two heating structures, each consisting of eight 1-m-long stainless-steel rods, connected by approximately 50 cm of flexible stainless-steel conduit. We used stainless-steel T-junctions at the top of each rod (adjoining the flexible conduit) and conical caps at the bottom of each rod. The final structure was 1.2 m tall. Inside each of the structures, we threaded 25 m of heating cable (SLMCAB10120BF, Briskheat) and filled the remaining space in the rods and conduit with quartz sand, selected for its high thermal conductivity. The complete structure was welded to seal the heating cable and sand inside. Two of these structures were buried around a 3.5-m-diameter circumference, with the top of the flexible conduit 5 cm belowground. Thus, each plot contained 50 m of heating cable inserted to 1.2 m depth, encircling a 3.5-m-diameter area, with an effective heated plot area of 5 m diameter. The experiment heats approximately 120 m³ of soil in total (five plots, 5 m diameter, 1.2 m depth). The plot design and heating methodology follows previous studies^{6,36}.

Experiment power supply

The experiment was powered using a 120-V supply, delivered from a mains outlet situated approximately 300 m from the experimental site. The power cables from the mains outlet to each of the five experiment control units were placed inside 19-mm-diameter liquid-tight flexible steel conduit and buried in roughly 20-cm-deep trenches. For each of the five control units (situated next to each warm-control plot pair), we installed a 20-A circuit breaker and a 12-V outlet, supplied by a battery connected to a 12-V battery maintainer. The 120-V outlets provided power to the heating cables, gas analyser system and battery maintainers; the 12-V outlet provided power to the dataloggers, relays and sensors. Maximum power consumption is 2,500 W (500 W per plot), although average consumption is roughly 500–1,000 W.

Temperature control

Each warming and control plot was connected to a thermostat system, which maintained soil temperature in the warmed plots at 4 °C above ambient temperature. The thermostat system consisted of three integrated temperature and moisture sensors per plot (CS655 Refractometer, Campbell Scientific; 20 cm in length), inserted to depths of 0–20 cm, 50–70 cm and 100–120 cm at the mid-radius point in each plot, which were connected to a control unit (one control unit for each plot pair; five in total). The CS655 sensors continuously measured soil temperature to control the thermostat and logged the soil temperature and volumetric soil moisture every hour. These whole-profile measurements were complemented by independent measurements of surface (0–20 cm) soil temperature and moisture (see below).

The control units consisted of waterproof (IP68) enclosures containing a solid-state power controller (DA10-24CO-0000, Watlow), relay (12-V single channel), datalogger (CR1000, Campbell Scientific), and 12-V and 120-V power supply. Temperature in each warmed plot was therefore maintained at 4 °C above the temperature in each corresponding paired control plot, based on the average temperature from 0 cm to 120 cm depth at the mid-radius point in each plot. The average temperature difference over two years was 3.96 °C, which corresponds to the average of 2.7 °C at 0–20 cm depth, 4.0 °C at 50–70 cm depth and 5.2 °C at 100–120 cm depth.

This experimental design has been shown to warm the soil approximately uniformly across the soil volume, with minor anomalies of warmer soil very close to the heating rods (within 10 cm) and slightly cooler surface soils as a result of heat-transfer to the air^{6,36}. Therefore, surface soils were slightly cooler compared to subsoils, although the response of surface soils (rather than subsoils) will probably dominate the warming response across the soil profile because they contain greater organic matter (two-thirds of the carbon stock occurs in the upper 50 cm of the soil profile; Extended Data Table 1). The heating structures were installed during May–July 2016, and plots were tested during June–October 2016. The testing phase consisted of heating each plot by 4 °C for approximately 2-week periods. The experiment was switched on in full on 1 November 2016.

Soil gas-exchange and partitioning

Soil CO₂ efflux was measured every two weeks from 2016 until 2019 at four systematically distributed locations within each plot using an infrared gas analyser (IRGA Li-8100; LI-COR Biosciences). The measurement period was increased to every week during seasonal transitions. The soil collars for CO₂ efflux measurements were assigned to zones within each plot ('centre 1', 'centre 2', 'side 1' and 'side 2') and were relocated randomly within each zone every three months, for long-term within-plot spatial independence. Soil CO₂ efflux was also measured every two weeks for four root-partition cores per plot (two root-exclusion and two root-ingrowth) to determine soil- and root-derived components of the CO₂ efflux. At the same time as soil CO₂ efflux measurements, we measured soil temperature (using a HI98509 thermometer probe; Hanna Instruments) and soil moisture (using a Thetaprobe; Delta-T) at 0–20 cm soil depth for a random location within a 1 m radius of each soil collar, or within the root-partition cores.

Root-exclusion cores were made from PVC tubing (30 cm height, 10 cm diameter) with a 1-μm nylon mesh base for drainage. Root-ingrowth cores (disturbance controls) had additional windows (around 340 cm²) covered with 2-mm mesh around the sides³⁵. In each plot, two root-exclusion cores and two root-ingrowth cores were buried within each plot, approximately 30 cm from the heating cable (where the soil profile is warmed on average by 4 °C).

The percentage contributions of fine roots and rhizo-microorganisms (root-derived) and free-living heterotrophic microorganisms (soil-derived) to the total soil CO₂ efflux were calculated as follows:

$$\text{soil-derived CO}_2 \text{ efflux (\%)} = (\text{root-exclusion core CO}_2 \text{ efflux}) / (\text{root-ingrowth core CO}_2 \text{ efflux}) \times 100, \quad (1)$$

$$\text{root-derived CO}_2 \text{ efflux (\%)} = 100 - \text{soil-derived CO}_2 \text{ efflux (\%)}. \quad (2)$$

Total soil CO₂ efflux measured for soil collars was multiplied by the results from equations (1) and (2) to estimate the absolute contributions of root-derived (roots, rhizo-microbial and mycorrhizal) and soil-derived (free-living microbial through the decomposition of litter and soil organic matter) components³⁷. The partition cores were buried to 0–25 cm depth, where 95% fine roots occur³⁸. Therefore, the soil

component consists of soil-derived CO₂ from the entire soil profile (with a minor contribution from fine roots at greater than 20 cm depth).

Soil properties

Soil was sampled before the experimental treatments began (to 100 cm depth; Extended Data Table 1) and then every three months after the beginning of the experiment (0–10 cm; average responses in Extended Data Fig. 5), at a point within the plots where the surface soil is heated evenly (at approximately 30 cm from the heating structure). These samples were then analysed using standard procedures to determine the soil properties: total elements, available nutrients, microbial carbon, nitrogen and phosphorus, and enzyme activities (see below). We calculated microbial CUE using microbial carbon, nitrogen and phosphorus and enzyme activity data using a stoichiometric method³⁹. Here we describe the responses following two years of warming, by using the average change in soil properties over two years (average of eight temporal measurements per plot, with $n = 5$ per plot).

Total carbon and nitrogen were determined simultaneously by automated combustion and gas chromatography using a Thermo Flash 1112 elemental analyser (CE Elantech). Total phosphorus was determined by ignition (550 °C, 1 h) and extraction in 1 M H₂SO₄ (16 h; 1:50 soil to solution ratio) with phosphate detection by automated molybdate colorimetry. Exchangeable cations were determined by extraction in 0.1 M BaCl₂ and detection by inductively coupled plasma-optical emission spectrometry with an Optima 7300 DV (Perkin-Elmer)⁴⁰. Effective cation exchange capacity (ECEC) was calculated as the sum of the charge equivalents of Al, Ca, Fe, K, Mg, Mn and Na. Soil pH was determined in deionized water in a 1:2 soil to solution ratio.

Extractable carbon and nitrogen were determined by fresh soil extraction in 0.5 M K₂SO₄. Soil microbial biomass carbon and nitrogen were measured by fumigation–extraction^{41,42}, using ethanol-free chloroform as the fumigant followed by extraction with K₂SO₄. Extracts of fumigated and unfumigated soil were analysed for extractable organic carbon and nitrogen using a TOC-VCHN analyser (Shimadzu). Microbial carbon and nitrogen were calculated as the difference in the respective nutrient between fumigated and unfumigated extracts and corrected for unrecovered biomass using a k factor⁴³ of 0.45. Microbial biomass phosphorus was determined by hexanol fumigation and extraction with anion-exchange membranes⁴⁴. Phosphate was recovered from anion-exchange membranes by shaking for 1 h in 50 ml of 0.25 M H₂SO₄, with detection in the acid solution by automated molybdate colorimetry using a Lachat Quikchem 8500 (Hach). Extractable phosphorus was determined on unfumigated samples and microbial phosphorus was calculated as the difference between the fumigated and unfumigated samples, with correction for unrecovered biomass using a k_p factor⁴⁴ of 0.4.

Soil enzyme activity (V_{max}) was determined for seven enzymes involved in carbon and nutrient cycling. We used microplate fluorimetric assays with 100 μM methylumbelliflone (MU)-linked substrates to measure the activity of β-glucosidase (degradation of β bonds in glucose), cellobiohydrolase (degradation of cellulose), N-acetyl β-glucosaminidase (degradation of N-glycosidic bonds), phosphomonoesterase (degradation of monoester-linked simple organic phosphates), sulfatase (degradation of sulfate esters) and β-xylanase (degradation of hemicellulose). For each soil sample, five replicate microplates were prepared and incubated at 2 °C, 10 °C, 22 °C, 30 °C or 40 °C to calculate the temperature sensitivity (Q_{10}) of V_{max} and determine V_{max} at control (26 °C) and warmed (30 °C) soil temperatures. Further information on protocols for enzyme analyses is provided elsewhere^{45,46}. All analyses apart from total elements (carbon, nitrogen, phosphorus), cations and pH were determined on fresh soils within 24 h of sampling, and K₂SO₄ extracts within 6 h, to avoid the rapid changes that can occur during storage or pretreatment⁴⁷. All soil chemical properties are expressed on the basis of oven-dry equivalent soil (determined by drying at 105 °C for 24 h).

Determination of carbon and nutrient use efficiencies

We estimated carbon, nitrogen and phosphorus use efficiencies (CUE, NUE and PUE) from ecological stoichiometry, whereby the CUE, NUE or PUE of an organism is a function of the difference between its elemental requirements for growth (carbon, nitrogen or phosphorus in biomass and enzymatic investment for acquisition) and the abundance of environmental substrate (carbon, nitrogen or phosphorus in soil organic matter). This approach assumes that enzyme activities scale with microbial production and organic-matter concentration, and that microbial communities exhibit optimum resource allocation with respect to enzyme expression and environmental resources. These assumptions are empirically supported by Michaelis–Menten kinetics and metabolic control analysis³⁹. On the basis of this underlying assumption, CUE is calculated as

$$CUE_{C:X} = CUE_{MAX}[S_{C:X}/(S_{C:X} + K_X)],$$

$$S_{C:X} = (B_{C:X}/L_{C:X})/EEA_{C:X}.$$

Here $S_{C:X}$ represents the extent to which the allocation of enzyme activities offsets the disparity between the elemental composition of available resources and the composition of microbial biomass. $K_X = 0.5$ and $CUE_{MAX} = 0.6$ are the half-saturation constant and the upper limit for microbial growth efficiency based on thermodynamic constraints, respectively. EEA_{C:X} is the extracellular enzyme activity (nmol g⁻¹ h⁻¹): EEA_{C:N} was calculated as BG/NAG, where BG = β-glucosidase and NAG = N-acetyl β-glucosaminidase, and EEA_{C:P} was calculated as BG/P, where P = phosphomonoesterase. Molar ratios of soil organic carbon to total nitrogen to total phosphorus were used as estimates of $L_{C:X}$. Microbial biomass ratios $B_{C:X}$ were also calculated as molar ratios.

Statistical analyses

Treatment (warming) effects on time-averaged total and partitioned CO₂ emissions and other soil properties (nutrients and microbial properties) were tested using ANOVA. Treatment effects on soil CO₂ emissions were primarily tested for using mixed-effects models with CO₂ efflux as the response variable, warming treatment, soil moisture, season, warming × soil moisture and season × soil moisture as fixed effects, and plot number as a random effect⁴⁸. As the within-plot location of the four soil CO₂ efflux sampling points (soil collar) was changed every three months, we did not include time as a random effect (repeated measures) in the primary model. The soil collars within each plot were moved every three months, but always systematically assigned to zones within the plot: centre 1, centre 2, side 1 and side 2. The soil collars were moved to avoid long-term disturbance of the soil due to the presence of the soil collar, and to ensure that the within-plot soil CO₂ efflux measurements were spatially independent in the long-term. To test whether this pattern of measurement frequency and soil-collar movement influenced our results, we also ran models using a repeated-measures approach, with both space (soil-collar zonal location, nested in plot) and time as random effects. This repeated-measures analysis reinforced the findings from the primary model analysis (Extended Data Table 2). To test the response of partitioned soil- and root-derived CO₂ emissions to warming, we used repeated-measures analyses because the partition cores were fixed, with plot number and time as random effects. Treatment effects on partitioned root- and soil-derived CO₂ efflux components were tested using repeated-measures mixed models with time and plot number as random effects.

Treatment effects on soil-surface moisture content (0–20 cm depth) were tested using mixed-effects models with volumetric soil moisture as the response variable, warming treatment, season and warming × season as fixed effects, and plot number as a random effect. In this case, we did not use a repeated-measures analysis because each within-plot soil-moisture sampling point was wholly independent.

Article

Treatment effects on whole-soil-profile moisture, which were repeated measures, were tested using a repeated-measures analysis with space (depth nested in plot) and time as random effects. All statistical analyses were performed in R (version 3.5.2).

Data availability

The source data for this study (soil gas exchange, soil and microbial properties) are available at <https://doi.org/10.6084/m9.figshare.12144768>. Source data are provided with this paper.

33. Leigh, E. G. J. *Tropical Forest Ecology: A View from Barro Colorado Island* (Oxford Univ. Press, 1999).
34. Woodring, W. P. Geology of Barro Colorado Island. *Smithson. Misc. Collect.* **135**, 1–39 (1958).
35. Sanchez, P. A. & Logan, T. J. Myths and science about the chemistry and fertility of soils in the tropics. *SSSA Spec. Publ.* **29**, 35–46 (1992).
36. Hanson, P. J. et al. A method for experimental heating of intact soil profiles for application to climate change experiments. *Glob. Change Biol.* **17**, 1083–1096 (2011).
37. Nottingham, A. T., Turner, B. L., Winter, K., van der Heijden, M. G. A. & Tanner, E. V. J. Arbuscular mycorrhizal mycelial respiration in a moist tropical forest. *New Phytol.* **186**, 957–967 (2010).
38. Cavelier, J. Fine-root biomass and soil properties in a semideciduous and a lower montane rain-forest in Panama. *Plant Soil* **142**, 187–201 (1992).
39. Sinsabaugh, R. L. et al. Stoichiometry of microbial carbon use efficiency in soils. *Ecol. Monogr.* **86**, 172–189 (2016).
40. Hendershot, W. H. & Duquette, M. A simple barium-chloride method for determining cation-exchange capacity and exchangeable cations. *Soil Sci. Soc. Am. J.* **50**, 605–608 (1986).
41. Brookes, P. C., Landman, A., Pruden, G. & Jenkinson, D. S. Chloroform fumigation and the release of soil-nitrogen – a rapid direct extraction method to measure microbial biomass nitrogen in soil. *Soil Biol. Biochem.* **17**, 837–842 (1985).
42. Vance, E. D., Brookes, P. C. & Jenkinson, D. S. An extraction method for measuring soil microbial biomass-C. *Soil Biol. Biochem.* **19**, 703–707 (1987).
43. Jenkinson, D. S., Brookes, P. C. & Powlsom, D. S. Measuring soil microbial biomass. *Soil Biol. Biochem.* **36**, 5–7 (2004).
44. Kouno, K., Tuchiya, Y. & Ando, T. Measurement of soil microbial biomass phosphorus by an anion-exchange membrane method. *Soil Biol. Biochem.* **27**, 1353–1357 (1995).
45. Nottingham, A. T. et al. Soil microbial nutrient constraints along a tropical forest elevation gradient: a belowground test of a biogeochemical paradigm. *Biogeosciences* **12**, 6489–6523 (2015).
46. Nottingham, A. T. et al. Temperature sensitivity of soil enzymes along an elevation gradient in the Peruvian Andes. *Biogeochemistry* **127**, 217–230 (2016).
47. Turner, B. L. & Romero, T. E. Short-term changes in extractable inorganic nutrients during storage of tropical rain forest soils. *Soil Sci. Soc. Am. J.* **73**, 1972–1979 (2009).
48. Zuur, A. F., Ieno, E. N., Walker, N. J., Saveliev, A. A. & Smith, G. M. *Mixed Effects Models and Extensions in Ecology with R* (Springer, 2007).

Acknowledgements This study was supported by two fellowships to A.T.N., a European Union Marie-Curie Fellowship FP7-2012-329360 (University of Edinburgh) and a Tupper Fellowship (Smithsonian Tropical Research Institute); a Smithsonian Institution Scholarly Studies Grant to B.L.T. and K. Winter; a UK NERC grant NE/K01627X/1 and an ANU Biology Innovation grant to P.M. We thank O. Acevado, D. Agudo, A. Bielnicka, M. Cano, D. Dominguez, M. Garcia, M. Larsen, B. Martin, M. Montero, S. O'Connor, J. Rodriguez, H. Szczegiel, I. Torres, W. Wcislo, K. Winter and S. J. Wright for their contributions to SWELTR.

Author contributions A.T.N. conceived the study with B.L.T. and P.M.; A.T.N., E.V. and B.L.T. performed the study. A.T.N. analysed the data and wrote the paper with B.L.T. and P.M.

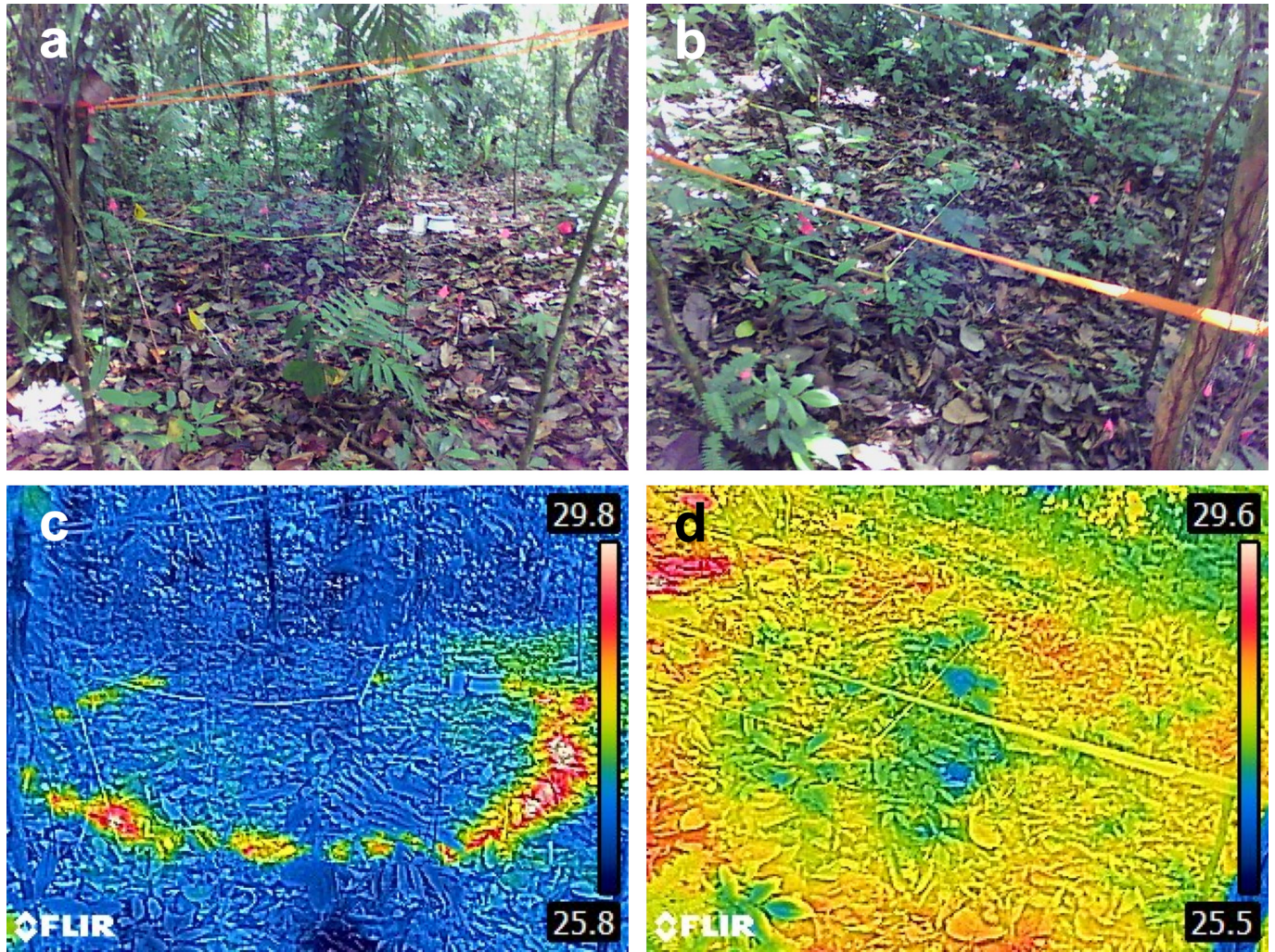
Competing interests The authors declare no competing interests.

Additional information

Correspondence and requests for materials should be addressed to A.T.N.

Peer review information *Nature* thanks Eric Davidson and the other, anonymous, reviewer(s) for their contribution to the peer review of this work.

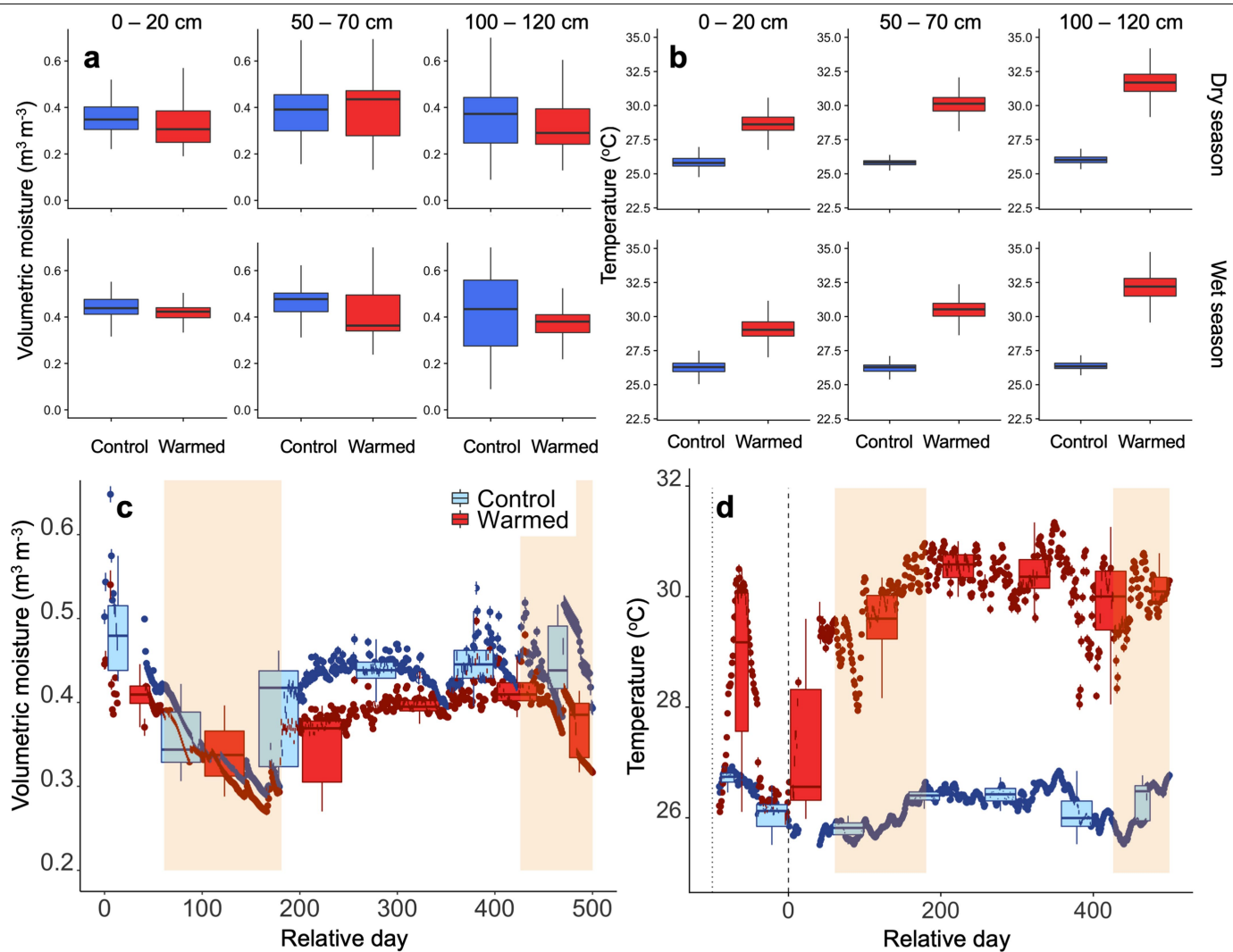
Reprints and permissions information is available at <http://www.nature.com/reprints>.



Extended Data Fig. 1 | Thermal images of a warmed plot. **a–d**, Pictures (**a, b**) and thermal images (**c, d**) of a warmed plot. The thermal images show the soil-surface temperature 1 h after the warming structure was switched on (**c**) and after a period of thermal equilibration of soil (**d**). The circular heating

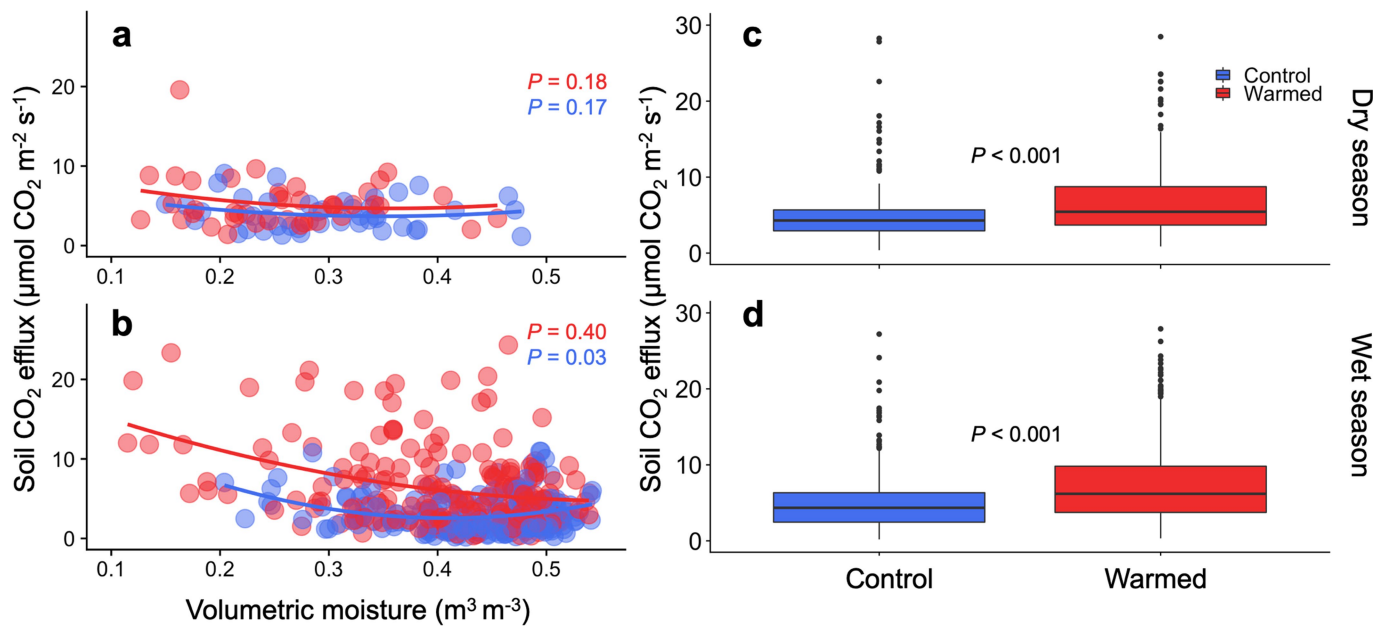
structure was 3.5 m in diameter and extended to 1.2 m depth, which resulted in an effective heated plot of approximately 5 m diameter and 1.2 m depth. The experiment consisted of five warmed and control plot pairs in total. Image credit: J. Bujan and E.V.

Article



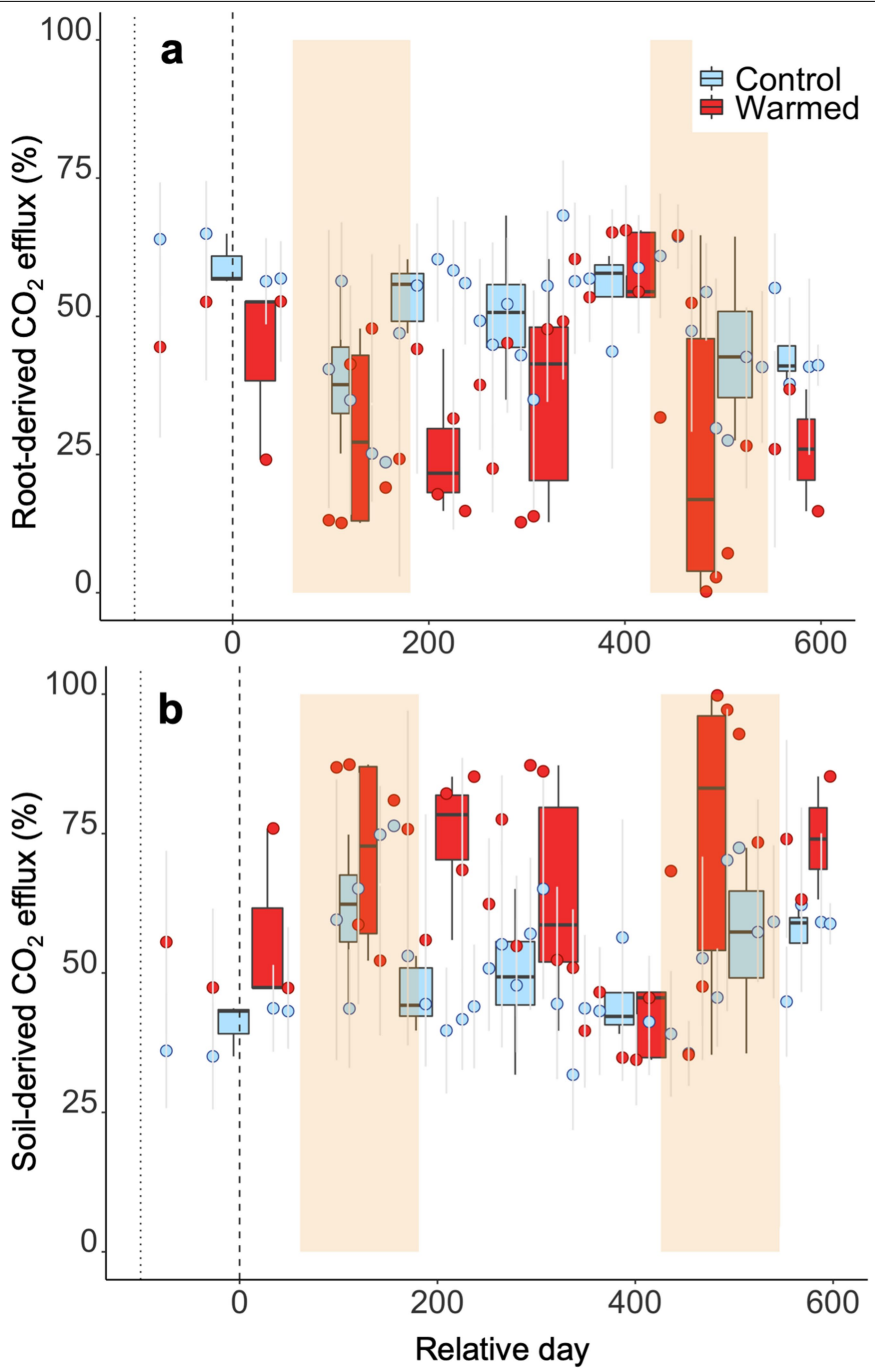
Extended Data Fig. 2 | Soil moisture content and temperature in control and warmed plots. **a, b**, Soil volumetric moisture content (**a**) and soil temperature (**b**), for the period after the warming treatment began (December 2016 to December 2018), partitioned by soil depth (columns) and season (rows). Box plots are standard (Tukey) plots, where the centre line represents the median across the five plots over the study period, the lower and upper hinges represent the first and third quartiles, and whiskers represent $+1.5$ the interquartile range. **c, d**, Temporal patterns in soil volumetric moisture content (**c**) and soil temperature (**d**), relative to when the warming treatment

began (relative day 0; temperature temporarily increased in warmed plots before this during the testing phase). The points are daily means of soil profile and the error bars represent one standard error of the variation by plot ($n=5$). The box (Tukey) plots show the median temporal value over sequential 100-day periods. The shaded areas represent dry seasons (1 January to 1 April). Treatment effects on annual or seasonal soil-profile moisture content were not significant; treatment effects on soil temperature were significant (repeated-measures ANOVA, $P < 0.001$; Extended Data Table 4).



Extended Data Fig. 3 | Relationship between soil CO_2 efflux, soil moisture and season, in control and warmed plots. a, b, Relationship between soil CO_2 efflux and soil moisture in warmed (red) and control (blue) plots during the dry (a) and wet (b) seasons. Data were fitted (solid lines) using a quadratic function. **c, d,** Soil CO_2 efflux differences between warmed (red) and control

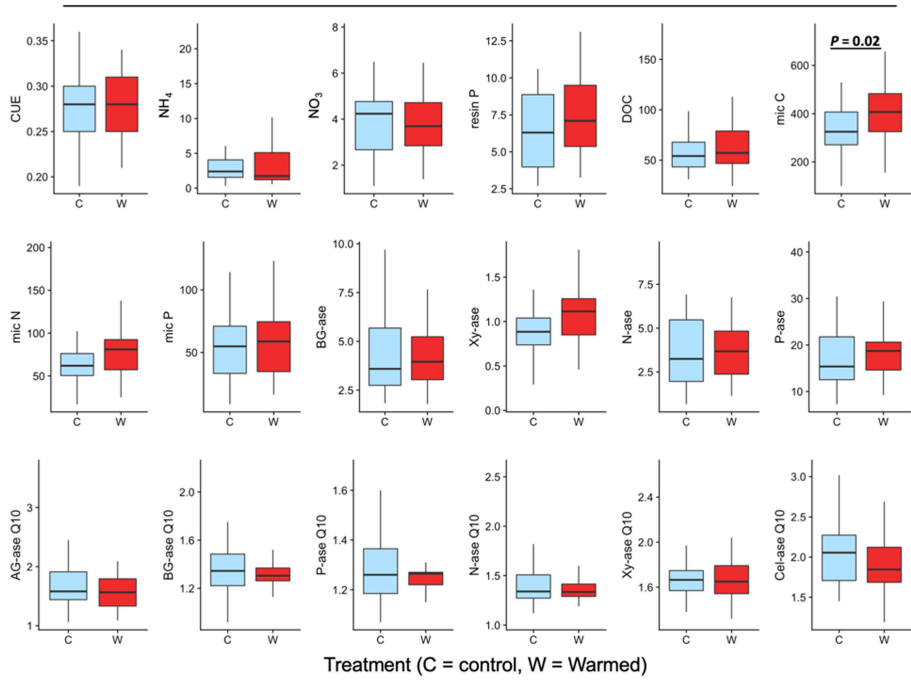
(blue) plots during the dry (c) and wet (d) seasons. Soil CO_2 efflux in warmed plots was significantly higher than controls for both dry and wet season, although the difference was greater for the wet season (average difference of $2.8 \mu\text{mol CO}_2 \text{ m}^{-2} \text{s}^{-1}$ for the wet season compared to $2.1 \mu\text{mol CO}_2 \text{ m}^{-2} \text{s}^{-1}$ for the dry season).



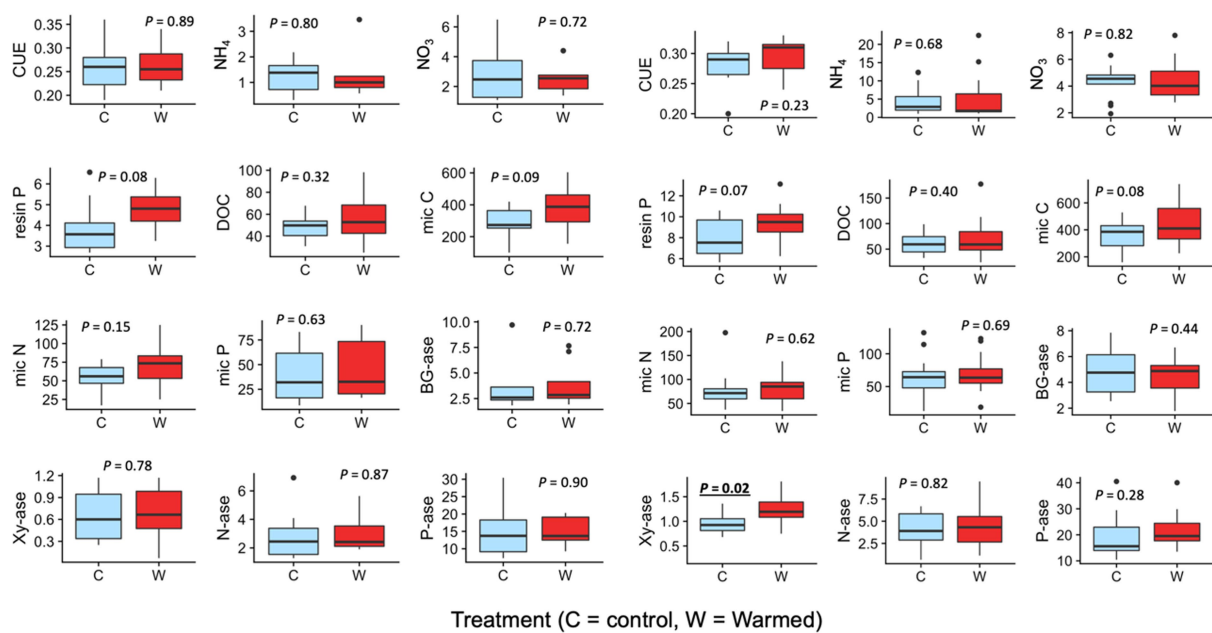
Extended Data Fig. 4 | Contribution of root-derived and soil-derived sources to total CO_2 efflux. **a, b,** Data for root-derived (**a**) and soil-derived (**b**) sources are for the study period. The error bars for points represent one standard error of the variation across the five plots. The box (Tukey) plots show the median temporal

value over 100-day periods. The dotted vertical line is when installation and testing of warming plots began; the dashed vertical line shows when all five warming plots were switched on permanently. The shaded areas represent dry seasons (1 January to 1 April).

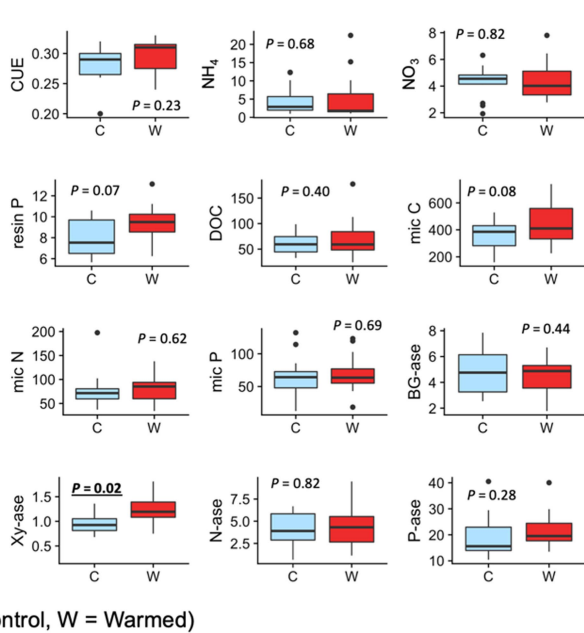
a Annual



b Dry season



c Wet season



Extended Data Fig. 5 | Average response of soil properties to warming.

a–c, Data are for the study period December 2016 to December 2018. Data are partitioned into annual (**a**), dry-season (**b**) and wet-season (**c**) responses. Soil properties are microbial CUE (ratio, no units), soil-extractable nutrients (NH₄, NO₃, resin P; mg kg⁻¹), dissolved organic carbon (DOC; mg kg⁻¹), microbial elements (mic C, mic N, mic P; mg kg⁻¹) and activities (V_{max}) of extracellular enzymes β -glucosidase (BG-ase), phosphomonoesterase (P-ase), N -acetyl β -glucosaminidase (N-ase) and β -xylanase (Xy-ase) (nmol MU g⁻¹ min⁻¹). The temperature sensitivity of activities of

extracellular enzymes (Q₁₀ of V_{max}) was determined for α -glucosidase (AG-ase), BG-ase, P-ase, N-ase, Xy-ase and cellobiohydrolase (Cel-ase) (nmol MU g⁻¹ min⁻¹). Significant responses ($P < 0.05$) are highlighted in bold and underlined. The only significant annual response (**a**) is for microbial carbon ($P = 0.02$), although there is also a marginal non-significant response for β -xylanase activity ($P = 0.07$). The centre line of each box plot represents the median across the five plots over the study period, the lower and upper hinges represent the first and third quartiles, and whiskers represent +1.5 the interquartile range.

Article

Extended Data Table 1 | Soil properties

Depth	0-10 cm	10-30 cm	30-50 cm	50-100 cm
C stocks (Mg C ha ⁻¹)	36.3 (3.3)	29.5 (1.5)	18.5 (1.0)	42.3 (3.3)
Total C (%)	3.63 (0.33)	1.34 (0.07)	0.77 (0.04)	0.65 (0.05)
Total N (%)	0.30 (0.02)	0.11 (0.01)	0.06 (0.00)	0.05 (0.00)
Total P (%)	0.34 (0.01)	0.20 (0.01)	0.14 (0.01)	0.11 (0.01)
K ₂ SO ₄ extractable - NH ₄ (mg N kg ⁻¹)	1.87 (0.27)	1.58 (0.10)	1.17 (0.24)	1.00 (0.17)
K ₂ SO ₄ extractable - NO ₃ (mg N kg ⁻¹)	1.38 (0.27)	0.35 (0.05)	0.15 (0.02)	0.12 (0.04)
Resin P (mg P kg ⁻¹)	1.40 (0.18)	0.90 (0.13)	0.40 (0.09)	0.61 (0.16)
ECEC (cmol _c kg ⁻¹)	48.8 (2.33)	49.1 (5.33)	42.90 (3.06)	42.4 (3.46)
Soil pH (H ₂ O)	6.02 (0.06)	6.04 (0.05)	6.00 (0.05)	6.02 (0.07)

Average values across soil depths for the study site (mean and standard error, $n = 10$). Resin P is phosphate extracted by anion-exchange membrane. ECEC, effective cation exchange capacity. Values are pre-treatment and were determined in 2015 before the warming experiment was installed.

Extended Data Table 2 | The determinants of soil CO₂ efflux variation

1. No repeated measures					2. With repeated measures						
a) Annual soil CO ₂ efflux		Parameter	SE	DF	P-value	a) Annual soil CO ₂ efflux		Parameter	SE	DF	P-value
<i>Fixed effects</i>											
Warming		3.23	1.50	13	< 0.05 *	Warming		2.66	0.97	89	< 0.01 **
Season		-0.55	0.76	521	0.48	Season		1.34	1.48	52	0.37
Soil moisture		-0.66	1.62	521	0.69	Soil moisture		0.48	1.87	196	0.80
Warming * soil moisture		-1.24	1.52	521	0.42	Warming * soil moisture		-0.46	1.23	494	0.71
Season * soil moisture		2.41	1.69	521	0.15	Season * soil moisture		-0.08	2.10	169	0.97
<i>Random effect</i>											
Space (plot number)		3.28	1.18	19	< 0.05 *	Intercept (Space + Time)		2.71	1.40	69	0.06
AIC value					2823	AIC value					2644
b) Wet season soil CO ₂ efflux		Parameter	SE	DF	P-value	b) Wet season soil CO ₂ efflux		Parameter	SE	DF	P-value
<i>Fixed effects</i>											
Warming		3.98	1.78	14	< 0.05 *	Warming		3.09	1.12	104	< 0.01 **
Soil moisture		2.43	1.34	2	0.07	Soil moisture		1.19	1.53	157	0.44
Warming * soil moisture		-2.06	1.90	424	0.28	Warming * soil moisture		-0.80	1.55	402	0.61
<i>Random effect</i>											
Space (plot number)		2.23	1.27	15	0.10	Intercept (Space + Time)		3.49	1.14	99	< 0.01 **
AIC value					2324	AIC value					2181
c) Dry season soil CO ₂ efflux		Parameter	SE	DF	P-value	c) Dry season soil CO ₂ efflux		Parameter	SE	DF	P-value
<i>Fixed effects</i>											
Warming		1.23	0.50	99	< 0.05 *	Warming		1.52	0.93	81	0.11
Soil moisture		-2.05	1.06	99	0.055	Soil moisture		-2.72	1.53	44	0.08
<i>Random effect</i>											
Space (plot number)		4.67	0.05	99	< 0.01 **	Warming * soil moisture		-0.78	1.96	74	0.69
AIC value					469	Intercept (Space + Time)		5.02	0.86	6	< 0.001 ***
						AIC value					465

The mixed-effect model analyses were performed with: (1) random effect of space (plot), that is, no repeated-measures effect; and (2) random effects of space (soil-collar location nested within plot) and time, that is, including the repeated-measures effect. We performed the analyses first including all annual data (a) and then partitioned by wet season (b) and dry season (c). We tested with and without a repeated-measures effect because within-plot soil CO₂ efflux measurements were partially spatially independent (within-plot locations of soil collars were changed every three months, but not on every two-week measurement occasion within each three-month period; when moved, soil collars were relocated to randomly specified locations, but always systematically assigned to zones). Mixed-effects models were fitted using maximum likelihood, by beginning with the full model (six variables: warming effect, soil moisture determined at 0–20 cm depth, season, interactions between soil moisture and warming and season, and random effects of space and time), followed by stepwise parameter removal. The final model was determined by lowest Akaike information criterion (AIC) value. For each parameter, the standard error (SE) and degrees of freedom (DF) are shown; significant values are in bold and highlighted by asterisks for P < 0.05 (*), P < 0.01 (**) and P < 0.001 (***)�.

Article

Extended Data Table 3 | Treatment effects on root and soil components of CO₂ efflux

Pre-treatment				
Root-derived CO₂	<i>Parameter</i>	<i>SE</i>	<i>DF</i>	<i>P-value</i>
<i>Fixed effects</i>				
Warming	1.01	4.34	8.0	0.82
<i>Random effect</i>				
Space (plot) + Time	13.13	3.65	9.0	< 0.001 ***
Soil-derived CO₂	<i>Parameter</i>	<i>SE</i>	<i>DF</i>	<i>P-value</i>
<i>Fixed effects</i>				
Warming	0.93	1.24	8.0	0.47
<i>Random effect</i>				
Space (plot) + Time	5.78	1.25	4.6	< 0.05 *
Post-treatment				
Root-derived CO₂	<i>Parameter</i>	<i>SE</i>	<i>DF</i>	<i>P-value</i>
<i>Fixed effects</i>				
Warming	2.4	1.82	8.0	0.21
<i>Random effect</i>				
Space (plot) + Time	3.6	1.34	9.4	< 0.05 *
Soil-derived CO₂	<i>Parameter</i>	<i>SE</i>	<i>DF</i>	<i>P-value</i>
<i>Fixed effects</i>				
Warming	2.90	0.98	8.0	< 0.05 *
<i>Random effect</i>				
Space (plot) + Time	3.47	0.79	12.8	< 0.001 ***

The flux components were derived from soil CO₂ efflux from root-ingrowth and root-exclusion cores. The mixed-effect model analyses were performed with random effects of space (plot) and time; a repeated-measures design was used because the partition cores were fixed. The analyses were performed including pre-treatment (January to June 2016) and post-treatment data following two years of warming (November 2016 to December 2018). For each parameter, the standard error (SE) and degrees of freedom (DF) are shown; significant values are in bold and highlighted by asterisks for $P < 0.05$ (*), $P < 0.01$ (**) and $P < 0.001$ (***)�.

Extended Data Table 4 | Determinants of soil moisture variation

1) Surface					
a) Annual soil moisture		Parameter	SE	DF	P-value
<i>Fixed effects</i>					
Warming		-0.05	0.04	84	0.19
Season		0.09	0.03	524	< 0.01 **
Warming * Season		0.02	0.04	524	0.64
<i>Random effect</i>					
Space (plot number)		0.39	0.02	84	< 0.001 ***
AIC value					-246
b) Wet season soil moisture		Parameter	SE	DF	P-value
<i>Fixed effects</i>					
Warming		-0.03	0.02	8	0.17
<i>Random effect</i>					
Space (plot number)		0.48	0.02	8	< 0.001 ***
AIC value					-268
c) Dry season soil moisture		Parameter	SE	DF	P-value
<i>Fixed effects</i>					
Warming		-0.06	0.05	98	0.25
<i>Random effect</i>					
Space (plot number)		0.39	0.03	98	< 0.001 ***
AIC value					469
2) Whole-profile					
a) Annual soil moisture		Parameter	SE	DF	P-value
<i>Fixed effects</i>					
Warming		-7.0×10^{-2}	5.8×10^{-2}	28	0.24
Season		0.15	6.8×10^{-3}	681	< 0.001 ***
Warming * Season		9.0×10^3	5.3×10^4	7.2×10^5	< 0.001 ***
<i>Random effect</i>					
Space (depth / plot) + Time (day)		0.42	4.2×10^{-2}	29	< 0.001 ***
AIC value					-11×10^5
b) Wet season soil moisture		Parameter	SE	DF	P-value
<i>Fixed effects</i>					
Warming		-0.05	0.07	28	0.44
<i>Random effect</i>					
Space (depth / plot) + Time (day)		0.57	0.05	28	< 0.001 ***
AIC value					-7×10^5
c) Dry season soil moisture		Parameter	SE	DF	P-value
<i>Fixed effects</i>					
Warming		-0.07	0.05	28	0.13
<i>Random effect</i>					
Space (depth / plot) + Time (day)		0.42	0.03	29	< 0.001 ***
AIC value					-6×10^5

Data are for (1) surface soils, 0–20 cm soil, measured by soil moisture probe; and (2) whole profile, 0–20 cm, 50–70 cm and 100–120 cm, measured by fixed moisture sensors. For surface soils (1), the analyses were performed including all data (1a) and then partitioned by wet season (1b) and dry season (1c). Mixed-effects models were fitted using maximum likelihood, by beginning with the full model (four variables in 1a: warming effect, season, and interactions between soil moisture and warming and season, and a random plot effect; two variables in 1b and 1c: as above but without seasonal effects) and then using step-wise parameter removal. All measurements of within-plot soil moisture were spatially independent. For whole-profile data (2), the analyses were performed including all data (2a) and then partitioned by wet season (2b) and dry season (2c). Mixed-effects models were fitted using maximum likelihood, by beginning with the full model (five variables in 2a: warming effect, season, and interactions between soil moisture and warming and season, and random effects of depth nested in plot and time; two variables in 2b and 2c: as above but without seasonal effects) and then using step-wise parameter removal. Repeated-measures analyses were used because the soil-profile moisture data are from fixed sensors. The final model was determined by lowest Akaike information criterion (AIC) value. For each parameter, the standard error (SE) and degrees of freedom (DF) are shown; significant values are in bold and highlighted by asterisks for $P < 0.05$ (*), $P < 0.01$ (**) and $P < 0.001$ (***)